Journal of Hydroscience and Hydraulic Engineering
Vol. 27, No.1 May, 2009, 71-81

MICROWAVE REMOTE SENSING OF LAND SURFACE STATUS DURING A LONG TERM EXPERIMENT, AND ITS APPLICATION TO VALIDATE A PARAMETER OPTIMIZATION METHOD

By

Hui Lu

The Department of Civil Engineering, The University of Tokyo, Bunkyo-ku, Tokyo, Japan

Toshio Koike

The Department of Civil Engineering, The University of Tokyo, Bunkyo-ku, Tokyo, Japan

Hiroyuki Tsutsui

The Department of Civil Engineering, The University of Tokyo, Bunkyo-ku, Tokyo, Japan

David Ndegwa KURIA

The Department of Civil Engineering, The University of Tokyo, Bunkyo-ku, Tokyo, Japan

Tobias Graf

The Department of Civil Engineering, The University of Tokyo, Bunkyo-ku, Tokyo, Japan

Kun Yang

Institute of Tibet Plateau Research, Chinese Academy of Sciences, Beijing, China

and

Xin Li

Cold and Arid Regions Environment and Engineering Research Institute, Chinese Academy of Sciences, Lanzhou, China

SYNOPSIS

Remote sensing, land surface modeling, and data assimilation are believed to yield an estimate of soil moisture and surface energy fluxes at various temporal and spatial scales. The aim of this study is to which aims to improve our understanding of the effect of land surface status on the microwave emission through a field experiment named 'Tanashi Experiment'. The scientific objectives are presented and the corresponding experiment set-up is described. The effects of soil moisture and vegetation layer on the brightness of various frequencies are analyzed. The

sensitivity of higher frequencies (18.7 and 36.5 GHz) on the soil moisture changing is also identified. A Land Data Assimilation System developed by the University of Tokyo (LDAS-UT) is validated by using data obtained from this experiment. And one important merit of LDAS-UT, parameter optimization, is verified through the comparison of optimized parameters with the in situ observed ones.

INTRODUCTION

Research related to earth system modeling, to global scale environmental processes monitoring and to climate change studying have been conducted using globally distributed parameters, such as the soil moisture, soil temperature and vegetation water content. Among them, the primary one is the soil moisture, which links the land surface and atmosphere by influencing the exchange of energy and material between these two parts. However, due to its large variability, it is very difficult to observe the spatial and temporal distribution of soil moisture on a large scale by means of in situ measurements, which are both time consuming and expensive. As a result, in the last 30 years, much effort has been made towards observing soil moisture by using satellite remote sensing approaches. Fortunately, satellite passive microwave remote sensing offers a possibility of measuring such an important variable on a global scale, by directly measuring the dielectric properties which are closely related to the liquid moisture content. Moreover, additional advantages of passive microwave remote sensing include long wavelength in the microwave region and independent of illumination source. Such characteristics have been recognized by many scientists and many research activities have been carried out in the past 30 years.

Currently, globally soil moisture products are mainly retrieved from C band and X band observation (1). In order to obtain time continuous information about soil moisture and land surface energy budget, land surface data assimilation systems have been developed. But there are still some problems that need to be solved, such as retrieving soil moisture from higher frequency bands (19GHz and 37GHz) observation which is installed on the Special Sensor Microwave Imager (SSM/I) (2,3), counting the vegetation effects on different frequencies, and the parameterization problems inside the land data assimilation systems.

In order to improve our understanding of the radiative transfer process taken place on the land surface and to improve our capability to model land surface processes, a long term field experiment was designed to monitor the growth cycle of winter wheat, and were carried out from November 2006 to June 2007 in the Field Production Science Center in Graduate School of Agricultural and Life Sciences in the University of Tokyo (UTFPSC), Tokyo, Japan.

In this paper, we present the objectives and the overall set-up of the 'Tanashi experiment'. Some radiometric characteristics of bare soil and winter wheat were explored through microwave observations at the frequencies operating by the Advanced Microwave Scanning Radiometers for EOS (AMSR-E) (4) (6.925GHz, 10.65GHz, 18.7GHz, 23.8GHz, 36.5GHz and 89GHz). Finally the LDAS-UT was driven by the observed meteorological forcing data. The parameter optimization capability of LDAS-UT is validated by comparing the retrieved land parameters with the observed ones.

EXPERIMENTAL DISCRIPTION

The 'Tanashi Experiment' was designed with the following two objectives in mind: (1) Improving our understanding of the effects of soil moisture change and vegetation development on the microwave emission at different frequencies and polarizations; and (2) Gaining a better understanding of the interaction processes between land surface and atmosphere, by means of the validation of LDAS-UT with in situ observed data set.

Site overview

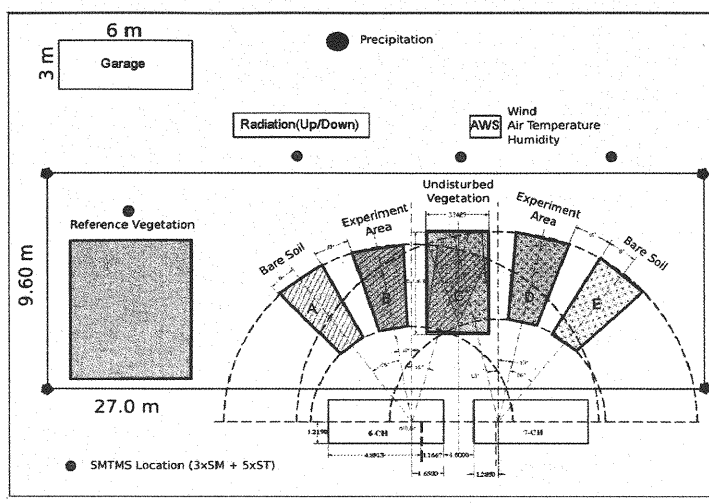

Figure. 1 Overview of Instrument Set-Up

Figure 1 shows an overview of the instrument set-up. Two Ground Based Microwave Radiometer (GBMR) systems, GBMR-6ch and GBMR-7ch, were installed at the edge of experiment field. In front of those two radiometers, there are 5 footprints which are the main targets of this field experiment.

Footprints A and B are the reference bare soil footprint and the reference vegetation footprint of GBMR-6ch, respectively. Analogously, footprints E and D are the reference footprints for another radiometer, i.e. GBMR-7ch. Footprint C, the one in the central location which can be observed by GBMR-6ch and GBMR-7ch simultaneously, is the common footprint.

Two different scan areas were selected to observe the brightness temperature of the field in different situations:

Footprints B,C and D – Undisturbed footprint: The plots in this area were undisturbed during whole observation period and, therefore it represented the natural status of the field.

Footprints A and E – Reference bare soil footprint: In this area the vegetation was removed regularly to keep the bare soil from being exposed to radiometers.

Beside these 5 footprints, there is a plot used as vegetation reference site. All of the vegetation sampling procedures were taken here to prevent disturbing the natural situation of footprint B, C and D.

The location for soil moisture and temperature measurement system (SMTMS) and the automatic weather station (AWS) were selected, so that they are close to the radiometer footprints. The radiation station and rainfall gauge were also placed close to the footprint to ensure the representativity of meteorological data measurement.

Brightness temperature observation

The ground based brightness temperature observations were implemented by means of the 6 channel Ground Based Microwave Radiometer (GBMR-6ch) and 7 channel Ground Based Microwave Radiometer (GBMR-7ch). The GBMR-6ch is a dual polarization, multi-frequency passive microwave radiometer, which observes the brightness temperature at 6.925, 10.65 and 18.7 GHz, while the GBMR-7ch operating at frequencies of 18.7, 23.8, 36.5 and 89GHz with both horizontal and vertical polarizations, with the exception of 23.8GHz which is vertical polarization only. A set of these two radiometers was developed to provide frequencies similar to those of the Advanced Microwave Scanning Radiometers for EOS (AMSR-E) on Aqua and AMSR on ADEOS-II. Details of GBMR-6ch and GBMR-7ch can be found in a previous paper of authors (5) and from manuals provided by the manufacturer, RPG (6).

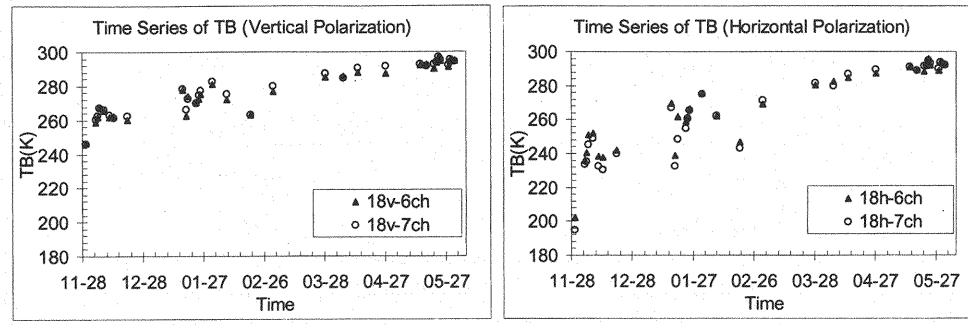

Figure. 2 Comparison of TB observed at 18GHz by GBMR-6ch and GBMR-7ch

Figure 2 shows a comparison between the brightness temperatures observed at 18.7 GHz by GBMR-6ch and that by GBMR-7ch. Closed triangle points represent the results measured by GBMR-6ch, and open circles are those measured by GBMR-7ch. The root mean square error between the GBMR-7ch and GBMR-6ch is 1.74K for vertical polarization (left figure), and 4.03K for horizontal polarization (right figure), respectively. Considering the fact that the calibration scheme is different for GBMR-6ch and GBMR-7ch, and the fact that the observed target is around 300K, such accuracy is acceptable. Thus, we are sure that both systems were able to observe the same target with the same degree of accuracy at the same time. Finally, a data set including brightness temperature measurements from 6.9GHz up to 89GHz is then created.

Soil temperature and moisture measurement

The Soil Moisture and Temperature Measurement System (SMTMS) was installed for simultaneous measurement of soil moisture and temperature profiles. The SMTMS used in this study have ten temperature probes and six soil moisture probes. Such probes were set at the following depths 0cm, 3 cm, 5 cm, 10 cm, 20 cm, 50 cm and 100 cm.

Soil samples were taken after every measurement to obtain data about the soil density and water content. An infrared thermometer was used to measure the temperature of soil surface and the temperature of vegetation surface.

Meteorological data measurement

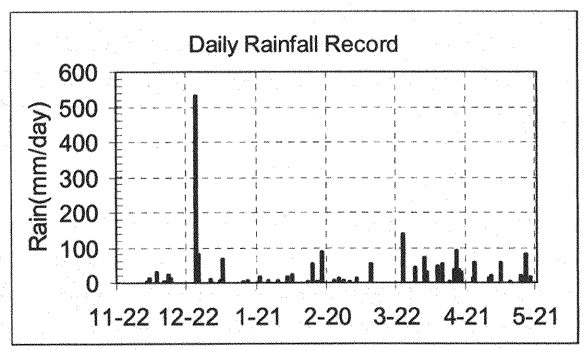

Figure. 3 Time series of daily rainfall

The automated weather station (AWS) was installed to continuously monitor the meteorological conditions at the site. The following items were recorded by AWS every 10 minutes: wind direction, wind speed, air temperature,

relative humidity, radiation (upward and downward of long wave and shortwave) and precipitation. Such atmospheric measurements are used to drive the Land Surface Data Assimilation System of the University of Tokyo (LDAS-UT).

Figure 3 shows a time series of daily rainfall. It was identified easily when a typhoon hit this field on December 26 in 2006 and brought a heavy rain of 531 mm. This extreme event changed the soil moisture content and the surface roughness dramatically, and also destroyed the TDR probes which resulted in the loss of continuous soil moisture profile measurements.

Soil texture and roughness data

The soil in the field is so-called 'Kanto loam', a typical soil in Tokyo area, with a sand fraction of 26% and a clay fraction of 43%. The observed soil bulk density is 0.587 g/cm^3 for the period before February 2007 and 0.606 g/cm^3 for period from March to June 2007.

The land surface roughness was measured by means of a pin profiler. Two roughness parameters *rms* height (h) and correlation length (l) were retrieved from roughness measurement. Since we were able to go into the field after the winter wheat had developed completely, there was no roughness measurement for vegetated plots after February.

Vegetation measurement

Vegetation development was monitored by measuring the height, biomass, dry matter, water content and area. Sampling area of 1*1 m^2 area was selected in the vegetation reference field. Wet biomass was measured just after cutting, and then the wheat was separated into three parts: heads, leaves and stems. Weight and area of each part were measured separately. By summing the area of those three parts, the Vegetation Area Index (VAI) was calculated.

A spectroradiometer, ASD FieldSpec Pro, was also used to measure the reflectance at a spectral range of 350nm - 2500nm. The normalized difference vegetation index (NDVI) was calculated by using reflectance values of red bands (620 - 670nm) and Near-Infrared (NIR) bands (841 - 876 nm), the same bands as MODIS products using.

According to the field observation, the vegetation water content (VWC) increased slowly during the period from November to March. However, after March, the vegetation developed rapidly. The entire experiment therefore can be divided into two periods: negligible vegetation effect period (before March) and vegetated period (after March 28).

OBSERVED RESULTS OF FIELD EXPERIMENTS

Observation results are discussed in this section, focusing on the new possibilities offered by the multi-frequency observation of the whole vegetation development process. First, the variability of brightness temperature to the variation of soil moisture is analyzed, from the low frequency of 6.9GHz up to the high frequency of 89GHz. Then the vegetation effects on different frequency observation are analyzed.

Soil moisture influents on the brightness temperature of different frequencies

Figure 4 shows the observed apparent emissivity (equals to the observed brightness temperature divided by the surface temperature) changing with various soil moisture content, for no vegetation effects period. The observation frequency of each panel is shown in the legend, for example, "6.9v_1" represents the observation at 6.9 GHz vertical polarization during the first period (before the typhoon), where "_2" means the observation during the second period (after the typhoon).

As mentioned in the section on meteorology data measurement, the typhoon changed the soil moisture and

surface roughness dramatically. As a result of it, the emissivity of low frequencies (6.925GHz, 10GHz and 18GHz) is separated into two groups (group 1 before typhoon and group 2 after typhoon). Also, the emissivity increased after typhoon occurred. This may have been due to the extreme weather event which changed the soil structure and the land surface roughness. Such situation is more obvious for horizontal polarization than for vertical polarization. The reason for this is that the horizontal signals are more sensitive to the surface roughness than the vertical ones are.

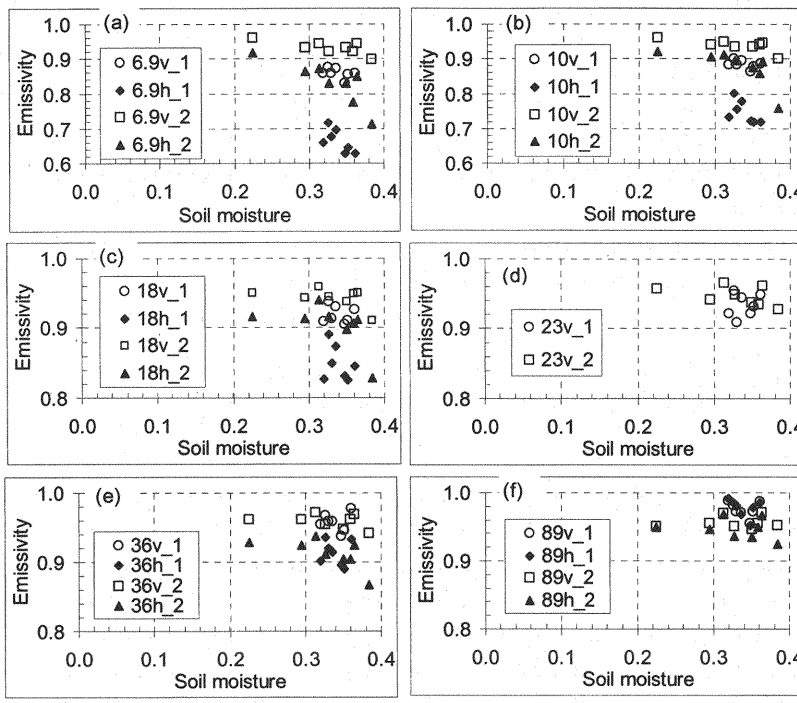

Figure. 4 Variation of emissivity at different frequencies according to the change of soil moisture, for no vegetation effects period. 'v' and 'h' represent the polarization. '_1' and '_2' represent the first period and the second period.

From Figure 4, one can easily see that the observed emissivity decreases as soil moisture increases for all horizontal polarization cases. This finding confirms previous studies (7, 8) and is in good agreement with the radiative transfer theory which builds on the basis of Dobson model and Fresnel equation for the wet soil cases (9-11).

Table. 1 Decrement of apparent emissivity due to the soil moisture increasing from 0.22 to 0.38

Pola. / F(GHz)	Vertical Polarization	Horizontal Polarization
6.925	0.06	0.21
10.65	0.06	0.16
18.7	0.04	0.09
23.8	0.03	N/A
36.5	0.02	0.06
89	0.00	0.02

Table 1 shows the decrement of the observed apparent emissivity due to the soil moisture increasing from 0.22 to 0.38. The decrement of emissivity is different for different frequencies and polarizations, with larger decrement for lower frequencies. From this table, it is clear that lower frequencies and horizontal polarization are sensitive to the soil

moisture changing. This finding provides strong support for using lower frequencies of AMSR-E to observe soil moisture from space. Moreover, findings show that there also exists some sensitivity for higher frequencies to the soil moisture changing. This means it is possible to retrieve soil moisture from high frequencies observation (e.g. 18.7 and 36.5 GHz), such as data of SSM/I and WindSat. Thus long term global soil moisture data can be estimated from long term SSM/I data which benefits research related to the climate change and global warming.

Vegetation effects on the apparent emissivity of different frequencies

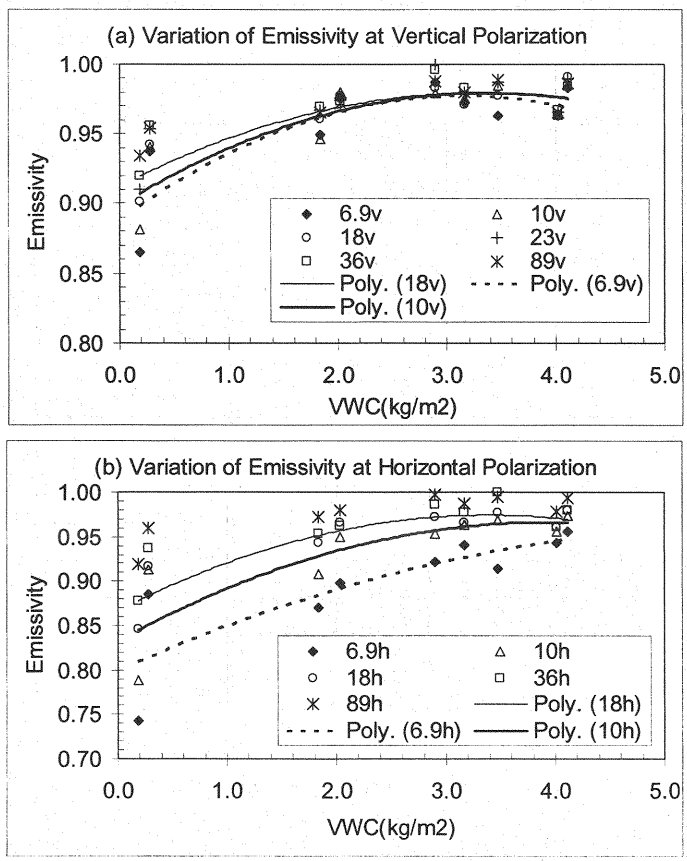

Figure. 5 Apparent emissivity responsive to the vegetation water content; 'v'and 'h' represents vertical and horizontal polarization. Thin lines denote the regression lines of 18GHz observation; the thick lines represent the regression lines of 10GHz; and the dash lines indicate the regression lines of 6.9GHz.

Figure 5 shows the changes of the apparent emissivity due to the increase of vegetation water content. From Figure 5, clearly shows that the apparent emissivity increases as vegetation water content increase. Finally, it becomes saturated and all frequencies and polarizations yield almost same values. For the cases of small VWC (such as VWC = 0.182 kg/m^2), the difference of apparent emissivity for different frequencies is large, giving 89GHz with largest values and 6.9GHz with smallest values. But for the cases when VWC is larger than 2.0 kg/m^2, it is hard to find such difference for vertical polarization case. For more vegetation water cases, all frequencies and polarizations observe almost same values. By comparing panel (a) with (b), especially for the 6.9GHz observation, it is clear that the emission from vegetation layer becomes dominant at the vertical polarization earlier than at the horizontal one.

By using Jackson's model (12), we can calculate the optical thickness (τ) and transmittivity (L) of vegetation layer as following equations:

$$\tau = b' \times \lambda^{\chi} \times VWC \quad (1)$$

$$L = \exp(-\tau / \cos\theta) \quad (2)$$

where λ = wavelength in cm, VWC = vegetation water content in kg/m^2, θ = incident angle, b' and χ are parameters dependent on the vegetation type. In the case of winter wheat, they are equal to 1.15 and -1.08, respectively.

Table 2 shows the calculation results of the transmittivity of vegetation layer on February 7, March 28, April 13 and May 17. From table 2, it is clear that the vegetation effect is small on February 7, with the evidence that the transmittivity is larger than 0.9 for lower frequencies. And after March 28, transmittivity is less than 0.5 for all frequencies. And as shown in figure 5, the regression line of 18GHz saturated when the VWC is larger than 2.0 kg/m^2; while the regression lines of 10GHz and 6.9GHz saturated at VWC around 4.0 kg/m^2. By summarizing the results shown in Figure 5 and table 2, the heavy vegetation criterion, over which the emission from vegetation layer is uniform for all microwave frequencies and polarization, is 2.0 kg/m^2 for frequencies higher than 18.7GHz. For all frequencies equipped on AMSR-E (including 6.925 and 10.65GHz), this criterion should move to 4.0 kg/m^2.

Table. 2 Transmittivity of vegetation layer

Date	Feb-07	Mar-28	Apr-13	May-17
VWC (kg/m^2) / F(GHz)	0.084	1.834	2.894	4.109
6.925	0.97	0.47	0.30	0.18
10.65	0.95	0.30	0.15	0.07
18.7	0.90	0.11	0.03	0.01
23.8	0.88	0.06	0.01	0.00
36.5	0.81	0.01	0.00	0.00
89	0.58	0.00	0.00	0.00

VALIDATION OF LDAS-UT

As mentioned in section 2, one of the main objectives of this long term experiment is to study the interaction between land surface and atmosphere. To accomplish this target, we ran LDAS-UT (13) to simulate soil variables (moisture and temperature profiles) and surface energy budget, by using in situ observed meteorological data as forcing data and GBMR TB data as observation data. As reported by Yang et al. (13), one important merit of LDAS-UT is its capability to optimize surface parameters by only using meteorological data and Brightness Temperature (TB) data. We therefore ran LDAS-UT in two scenarios: one running with in situ observed surface parameters and another running with optimized parameters produced by LDAS-UT itself.

Figure 6 shows a comparison between assimilated soil moisture and in situ observed one. The red line, marked as "DA_Opt", represents the assimilated results by using optimized parameters; the Green line, marked as "DA_Obs", represents the simulation result by using observed parameters; the circles, marked as "Obs", are the in situ soil moisture observed by can samples; and the purple columns represent the hourly rainfall. It is clear that both simulation scenarios agree well with the field observation, while the simulation with optimized parameter estimates soil moisture

a little higher than the simulation with observed parameters does. This overestimation is due to the setting of initial soil moisture values. For observed parameters simulation case, the observed soil moisture was used as initial value, while the initial value is much larger for optimized parameter simulation case. The RMSE of optimized parameter simulation is 0.045 and a little larger than that of observed parameter simulation which is 0.026.

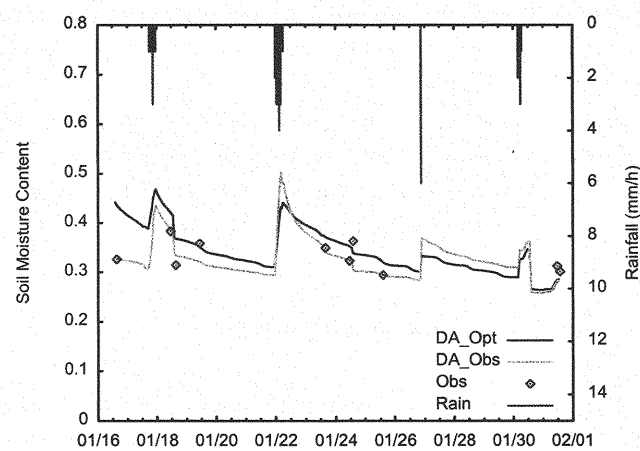

Figure. 6 Comparison between assimilated soil moisture and in situ observed one in 2007

Table 3 shows a comparison between optimized parameters and observed parameters. Generally speaking, the difference between two sets of parameter is not so large. The optimized soil texture parameters are very close to the observed ones. This means that the models used for accounting soil texture effects in LDAS-UT are in good agreement with physical facts. The optimized porosity is less than the observed one. This may be due to the measurement errors which overestimate the porosity or due to the limitation of current models in which the organic materials are not accounted. And the same situation is observed for the roughness parameters case. The difference between the optimized parameters and the observed ones reveals the potential source of uncertainty in the system due to the limitation of current RTM and LSS. However further research should be conducted to address on those parameters.

Table 3. Comparison between optimized parameters and observed parameters

	Optimized	Observed
SAND (%)	28.3	26
CLAY (%)	34.9	43
Porosity	0.587	0.778
rms h (cm)	0.513	1.01
l (cm)	0.478	1.16
www1	0.45	0.327

NOTE: www1 represents the soil moisture content of the first soil layer in the land surface model of LDASUT, the Simple Biosphere Model (SiB2) (14) (0-5cm)

SUMMARY

The 'Tanashi Experiment' is the first long term field experiment with TB measurement at all frequencies equipped on AMSR-E. This experiment was designed to couple the land surface process study and microwave radiative transfer model development, simultaneously. The data set made by this experiment makes it possible to examine the land surface radiative transfer process at various frequencies. Also, it can be used to validate land surface

scheme and data assimilation system.

From the no vegetation effects period, the observation results at lower frequencies are in accordance with former studies. Moreover, findings show that the higher frequencies also have some sensitivity to the soil moisture variation. This new finding encourages us to retrieve soil moisture from high frequencies observation data set, such as SSM/I and WindSat. By analyzing the experiment results during the vegetated period, the vegetation effects on various frequencies were revealed. It is found that the heavy vegetation criterion is 2.0 kg/m^2 for frequencies higher than 18 GHz and is 4.0 kg/m^2 for all AMSR-E frequencies.

By using in situ observed meteorological forcing data and TB data observed by GBMR, the capability of LDAS-UT was validated from the fact that its soil moisture estimation was in good agreement with in situ observation, no matter what observed parameters or optimized parameters were used. The difference between the optimized parameters and the observed ones revealed a potential source of uncertainty in the system. This matter should be addressed further.

ACKNOWLEDGMENT

This study was carried out as part of the Coordinated Enhanced Observing Period (CEOP) and Verification Experiment for AMSR/AMSR-E funded by the Japanese Science and Technology Corporation for Promoting Science and Technology Japan and the Japan Aerospace Exploration Agency. The authors express their great gratitude to them.

Furthermore, we would like to thank UTFPSC, for providing us the opportunity to conduct the field experiments on the university farm, Prof. Yonegawa and Mr. Kuboda for his helping in field management.

REFERENCES

1. Njoku, N. G., Jackson, T. J., Lakshmi, V., Chan, T. K., and Nghiem, S. V: Soil moisture retrieval from AMSR-E, IEEE Transactions Geoscience and Remote Sensing, Vol.41, pp.215-229, 2003.
2. Hollinger, J. P., Peirce, J. L., and Poe, G. A.: SSM/I Instrument Evaluation, IEEE Transactions on Geoscience and Remote Sensing, vol.28, pp.781-790, 1990.
3. Ridder, K. D.: Surface soil moisture monitoring over Europe using Special Sensor Microwave/Imager (SSM/I) imagery, Journal of Geophysical Research-Atmospheres, vol.108, 2003
4. Kawanishi, T., Sezai, T. , Ito, Y., Imaoka, K., Takeshima, T., Ishido, Y., Shibata, A., Miura, M., Inahata, H., and Spencer, R. W.: The Advanced Microwave Scanning Radiometer for the Earth Observing System (AMSR-E), NASDA's contribution to the EOS for global energy and water cycle studies, IEEE Transaction on Geoscience and Remote Sensing, vol.41, pp.184-194, 2003
5. Lu, H., Koike, T., et al: A Basic study on soil moisture algorithm using ground-based observations under dry condition, JSCE, Vol.50, 2006.
6. Technical documents of Radiometer Physics GmbH: Description 6 channel radiometer, Meckenheim, Germany. May, 1996.
7. Njoku, E. G.: Theory for passive microwave remote sensing of near-surface soil moisture, Journal of Geophysical Research, vol.82, pp.3108-3118, 1977.
8. Jackson, T. J., ONeill, P. E., and Swift, C. T.: Passive microwave observation of diurnal surface soil moisture, IEEE Transactions on Geoscience and Remote Sensing, Vol.35, pp.1210-1222, 1997.
9. Ulaby, F. T., Moore, K. T. and Fung, A. K.: Microwave Remote Sensing: Active and Passive, Volume III: From Theory to Application, Artech House Publishers, 1986.
10. Dobson, M. C., Ulaby, F. T., Hallikainen, M. T., and El-Rayes, M. A.: Microwave dielectric behavior of wet

soil—part II: dielectric mixing models, IEEE Transactions on Geoscience and Remote Sensing, Vol.GE-23, No.1, pp.35-46, 1985.

11. Ray, P. S.: Broadband complex refractive indices of ice and water, Applied Optics, Vol.11, No.8, pp.1836-1844, 1972.
12. Jackson, T. J. and Schmugge, T. J.: Vegetation effects on the microwave emission of soils, Remote Sensing of Environment, Vol.36, pp.203-212, 1991.
13. Yang, K., Watanabe, T., et al: An auto-calibration system to assimilate AMSR-E data into a land surface model for estimating soil moisture and surface energy budget, JMSJ, Vol.85A, pp229-242, 2007.
14. Sellers, P. J., Randall, D. A., Collatz, G. J. et al.: A revised land surface parameterization (SiB2) for atmospheric GCMs. Part I: model formulation. Journal of Climate, Vol.9, pp.676–705, 1996.

(Received Jul 31, 2008 ; revised Feb 25, 2009)